Electronic Supplementary Material (ESI) for Journal of Materials Chemistry C.

Laser irradiation-induced modification of the amorphous phase in GeTe films : The role of intermediate Ge-Te bonding in the crystallization mechanism

Seung Jong Park[a], Hanjin Park[b], Moon Hyung Jang[c], Min Ahn[a], Won Jun Yang[a], Jung Wha Han[a], Hong-Sik Jeong[d], Cheol-Woon Kim[b], Young-Kyun Kwon[*b], and Mann-Ho Cho[*a]

[a]*Institute of Physics and Applied Physics, Yonsei University, Seoul 120-749, Republic of Korea*

[b]*Department of Physics and Research Institute for Basic Sciences, Kyung Hee University, Seoul, 130-701, Republic of Korea*

[c]*Department of Material Science and Engineering, University of Pennsylvania, Philadelphia 19104, USA*

[d] *School of Integrated Technology, Yonsei University, Incheon 406-849, Republic of Korea*

S1. RBS analysis for atomic concentration in the as-grown amorphous GeTe film.

* To whom correspondence should be addressed. E-mail: ykkwon@khu.ac.kr & mh.cho@yonsei.ac.kr

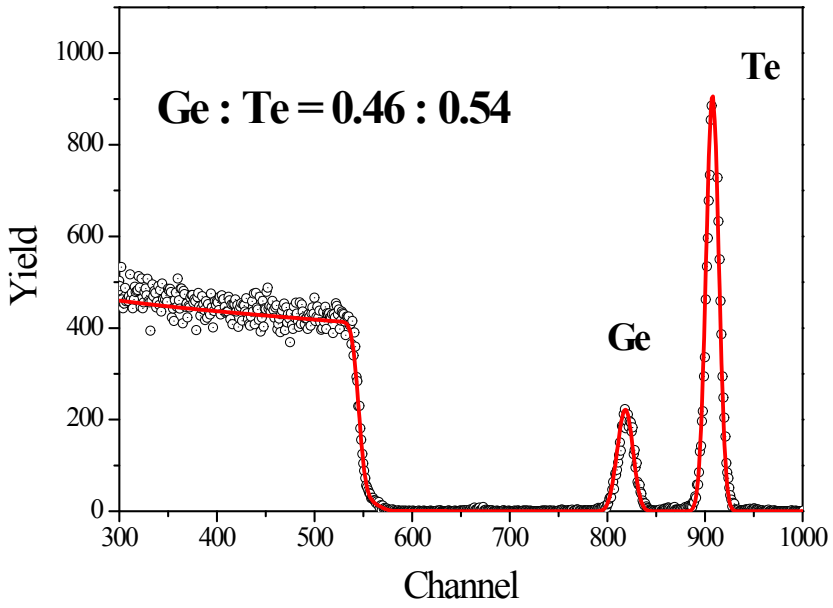

The RBS spectrum (open circle) of the as-grown amorphous GeTe. The fitting result (solid line) as a $Ge_{0.46}Te_{0.54}$ was analyzed by RUMP, which indicates the formation of a stoichiometric GeTe phase with uniform distributions of constituent atoms.

S2. The confirmation on formation of amorphous and crystalline phases.

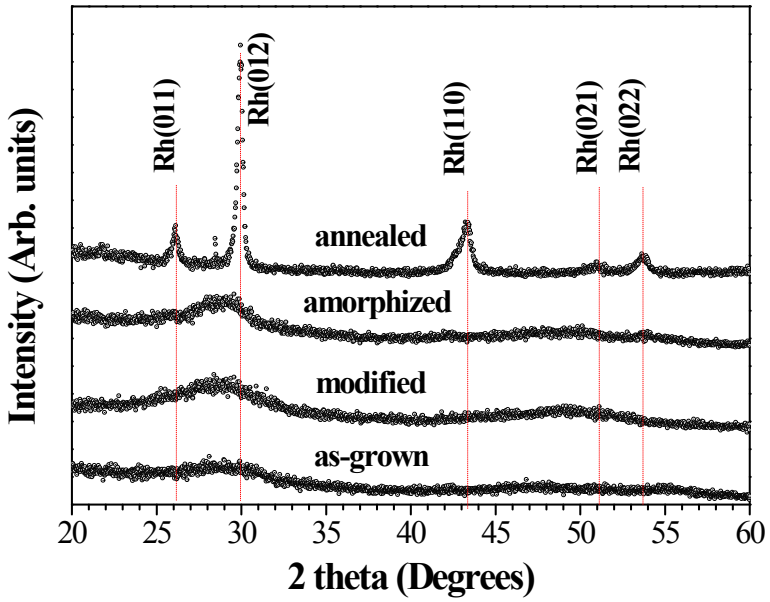

Figure S2. X-ray diffraction patterns of the amorphous and crystalline phases. The irradiated film (i.e., modified and amorphized films) show typical hollow patterns, indicating the formation of an amorphous phase without any long range order.

S2. Structural Analysis using Raman and XAFS.

Table S1. The Raman fitting parameters of the as-grown, irradiated and annealed GeTe films.

Sample	Fitting Parameter	Peak identity					
		I	II	III	IV	V	VI
As-grown	Frequency (cm^{-1})	80	111	128	159	219	259
	FWHM (cm^{-1})	32	19	19	57	35	48
	Contribution (%)	32	15	8	32	7	6
Modified amorphous	Frequency (cm^{-1})	81	111	126	158	216	256
	FWHM (cm^{-1})	28	22	21	38	41	42
	Contribution (%)	30	17	15	30	7	1
Sample	Fitting Parameter	Peak identity					
		I	II	III	IV	V	VI
Crystallized structure	Frequency (cm^{-1})	83	117	132			
	FWHM (cm^{-1})	28	26	61			
	Contribution (%)	46	33	20			
Amorphized structure	Frequency (cm^{-1})	79	111	126	158	216	256
	FWHM (cm^{-1})	28	19	19	40	41	42
	Contribution (%)	26	14	14	37	8	1

In the case of amorphous GeTe, the Raman modes were primarily characterized by the tetrahedral bonding structure of Ge and two-fold Te chains. In the fitting process, six Gaussian curves, denoted as I, II, III, IV, V and VI, were used to describe the spectrum between 60 and 300 cm^{-1}. This agrees with previous Raman studies.[1, 2] Since the phonon lifetime of the disordered material is a random distribution, as opposed to a finite value, the line shape of the Raman mode can be described by a Gaussian contribution.

Table S2. EXAFS fitting parameters of as-grown, irradiated, and annealed GeTe films.

	Bond	R (Å)	N	σ^2	ΔE_0(eV)
As-grown	Ge-Te	2.64(2)	1.75(35)	0.0087(20)	7.9(1.6)
	Ge-Ge	2.48(1)	1.81(34)	0.0044(14)	
Modified amorphous	Ge-Te	2.62(1)	1.67(38)	0.0066(21)	7.9 (set)
	Ge-Ge	2.49(1)	1.72(58)	0.0065(31)	
Crystallized Strucuture	short Ge-Te	2.792 (30)	2.42 (1.45)	0.0118 (70)	7.6 (3.4)
	long Ge-Te	3.128 (58)	2.83 (4.49)	0.0241 (367)	
	Ge-Ge	2.438 (27)	0.75 (54)	0.0041 (46)	
Amorphized Strucsture	long Ge-Te	3.30(4)	0.31(79)	0.0021(126)	7.6 (set)
	Ge-Ge	2.47(2)	1.76(78)	0.0052(33)	
	Ge-Te (amorphous)	2.63(4)	1.66(65)	0.0081(36)	

The extended X-ray absorption fine structure (EXAFS) fitting process for the Ge k-edge was conducted based on the single scattering path using Feff8.4 code. For the fitting process, the cluster molecular model containing tetrahedral and octahedral geometry was used as the initial fitting model that is specified as a cluster radius of 4.24 Å. The model calculation for the scattering path was carried out using an *ab initio* self-consistent field potential. In addition, the amplitude reduction factor (S_0^2 = 0.8) was acquired from a Ge reference foil, which satisfies the correlation between S_0^2 and σ^2 with various k weights (k^1 - k^3). The interatomic distance, coordination number, second (σ^2) and third (anharmonicity) cumulant were fitted for the Ge-centered bonding pairs using the calculated values such as the effective scattering amplitude, phase shift and mean free path. In particular, the third cumulant C_3 was included to consider the possibility of anharmonicity arising in the modified amorphous GeTe. The effective distance distribution $P(r, \lambda) = p(r)e^{-2r/\lambda}r^{-2}$ can be represented by the cumulant expansion, as introduced in a

previous study.[3] The C_3 cumulant is related to the anharmonicity by comparison to a Gaussian distribution of the interatomic distance. Each bond distance of Ge-Ge and Ge-Te bonding pairs were adjusted to minimize reduced Chi-square error, value less than 10. At the same time, the fitting process allows the common shift of the energy origin ΔE from initial E_0 for Ge-Ge and Ge-Te bonding pairs, respectively.

The EXAFS fitting parameter based on the single scattering path of Ge-Ge and Ge-Te bonding pairs is summarized in the supplementary information (Table S1). The non-zero value of the C_3 cumulant (0.00064±0.00037 $Å^3$) for Ge-Te bonding indicates the presence of asymmetric anharmonicity for the bonding distribution. Moreover, the mean-square relative displacement or C_2 cumulant (0.0053±0.0028 $Å^2$) of Ge-Te bonding in the modified amorphous phase has been defined as a lower value compared to the as-grown amorphous phase (0.0074±0.0068 $Å^2$). These changes induced by irradiation are simultaneously accompanied by a decrease in the coordination number (reduced from 3.56 to 3.39, which can be connected with the enhanced octahedral-like geometry in the Raman results.

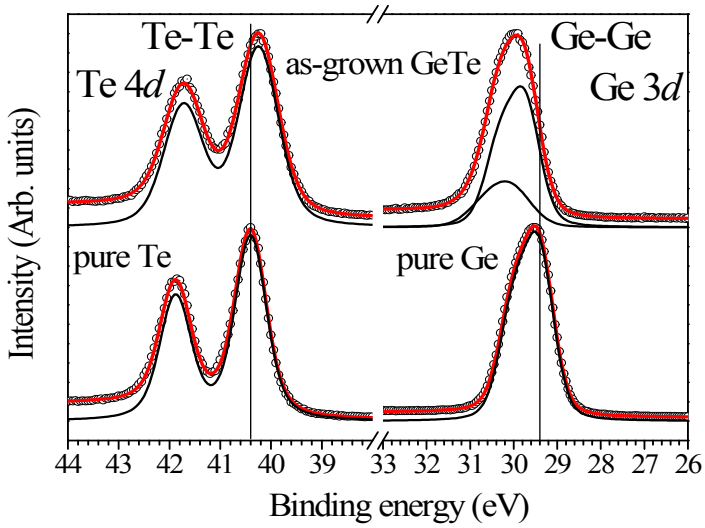

Figure S3 Using X-ray photoemission spectroscopy (XPS), the chemical bonding state of Ge in as-grown GeTe is compared with that in pure Ge.

X-ray photoemission spectroscopy (XPS) is typically useful for investigating discrepancies between homopolar and homo-/heteropolar mixtures of bonding structures. The pure-bonding and mixture-bonding structures in tetrahedrally bonded materials (group IV alloys) are precisely separated from the purely tetrahedral bonding structure.[4] Alternatively, the bond length is maintained under distributions of the homo-/heteropolar bonding structures. *In situ* XPS analysis clearly shows that there is no pure Ge-Ge homopolar bonding structure as shown in figure S3, and only Ge-Te bonding structures with different environments exist. Therefore, the Ge-Ge homopolar bonding based on EXAFS originates from the tetrahedral $GeTe_{4-n}Ge_n$ bonding structures.

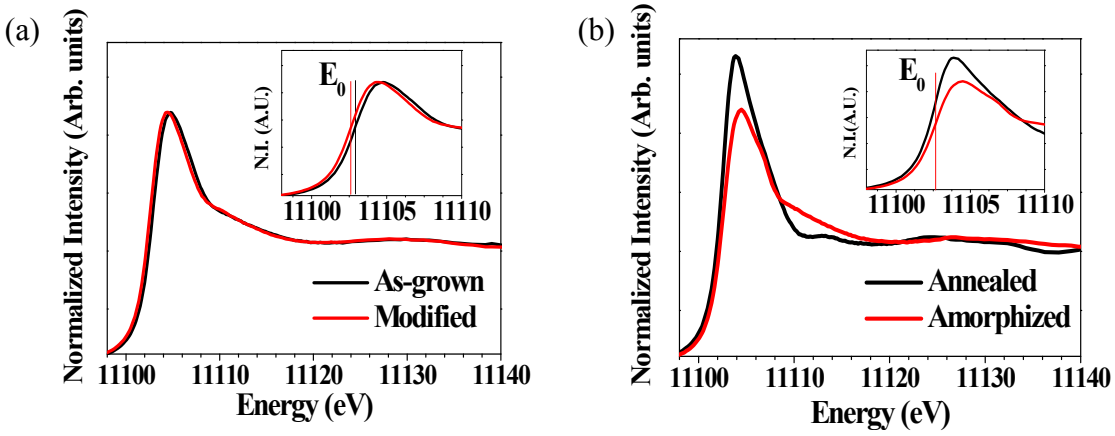

Figure S4. XANES spectra of the Ge k-edge for (a) as-grown and (b) annealed phases (including each irradiated phase) in GeTe films. In the case of the irradiated film, the E_0 of the absorption edge commonly shifts by 0.3 eV in the lower energy direction (relative to the as-grown phase). This indicates the formation of a pyramidal symmetry.

In order to investigate the transition of Ge bonding symmetry between the octahedral and tetrahedral structures, a XANES spectrum of the Ge k-edge was obtained. Figure S4 shows the normalized XANES spectrum of the Ge k-edge for the as-grown and modified phases. The white-line intensity and the slope of the shoulder around the high energy side in the XANES spectrum show distinct characteristics between octahedral and tetrahedral local structures.[5, 6] The octahedral local structure in the crystalline phase has a relatively higher white-line intensity and a lower slope than the tetrahedral local structure.[7, 8] Alternatively, the pyramidal structure deviates slightly from the tetrahedral symmetry of the Ge-centered local structure.[8] The XANES spectrum of the modified amorphous phase is nearly identical to that of the as-grown phase, but shows a slight shift to a lower energy (of 0.3 eV), which is close to the E_0 of the crystalline phase. The energy shift without deformation of the white-line shape indicates that the tetrahedral structure can more easily be transformed into a pyramidal structure with a p^3 bonding orbital than into an octahedral structure. Likewise, in the case of the amorphized phase, the white-line shape and the shoulder slope are nearly identical to the as-grown amorphous phase; the E_0 remains the same as that of the crystalline phase (i.e., a lower value than that of the as-grown amorphous phase). Although the

XANES spectra of the Ge k-edge cannot sensitively probe the difference between the modified and amorphized phases (i.e., the presence of a second type of Ge-Te bonding), it still provides insight into the possibility of the formation of a local pyramidal structure with a p^3 bonding orbital. With respect to the bonding orbital, it is interesting to investigate how the presence of the p^3 bonding orbital in the amorphous phase affects crystallization because the crystalline phase is purely composed of the p^3 bonding orbital. The Raman and XANES spectra show a strong similarity between the modified and amorphized phases. However, the EXAFS analysis showed a possible discrepancy with respect to the second type of Ge-Te bonding between both phases.

S3. Computational analysis based on Molecular dynamics simulation.

To explore three different amorphous phases of GeTe, i.e., as as-grown, modified and amorphized phases, which were observed to exhibit distinguishable characteristics, we performed various MD simulations with the three different initial structures we had modeled. The initial configurations for the as-grown and irradiated phases were constructed such that their respective nearest neighbor bonding distances between Ge-Te and Ge-Ge, and the coordination number (CN) of each element are consistent with our EXAFS data. With these initial structures, we carried out constant-temperature MD simulations at $T = 300\,K$ to equilibrate the structures. To obtain the amorphized phase, on the other hand, we commenced MD-based melt-quench simulations with its corresponding crystalline phase to mimic a real amorphization process. To reduce computational cost, we first executed MD simulations at a high temperature (5000 K) and with a low density ($\approx 5\,\%$ lower than its normal density by expanding the original unit cell), called pre-melting process, to scatter atoms from their equilibrium positions in the optimized crystalline phase. We then continued our MD simulations with the original density obtained by scaling down the structure at $T = 1000\,K$ to mimic its liquid phase. After the structure reached equilibrium at $T = 1000\,K$, a quenching process was employed with a rate of 10 K/ps until the system reached room temperature (300 K). During every MD simulation, we collected the coordinates $\{r_i\}$ and velocities $\{v_i\}$ $(i = 1, 2, 3, \cdots)$ of all atoms, with which we analyzed their various structural properties.

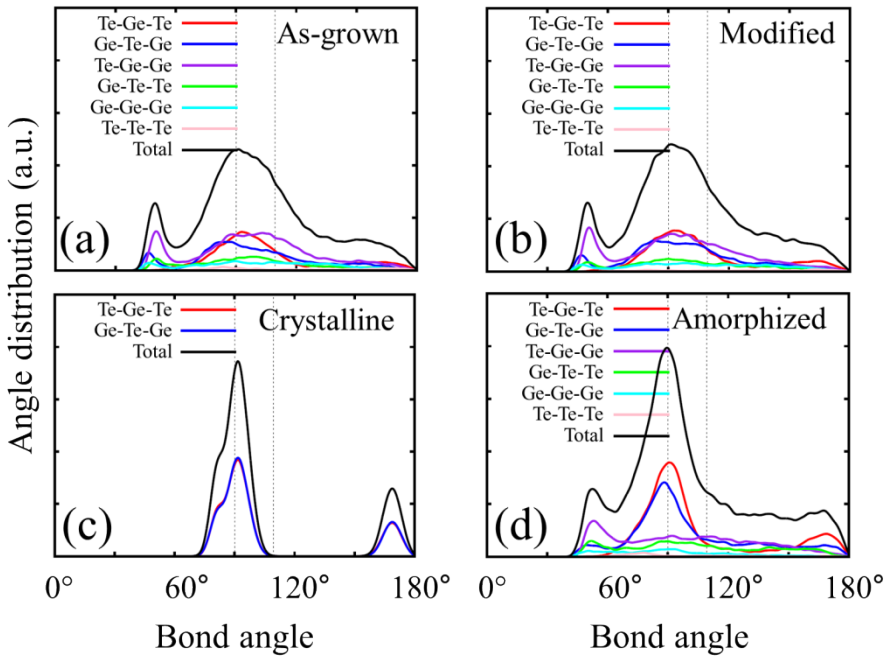

Figure S5. Angular distribution of the as-grown (a), the modified (b), the crystalline (c), and the amorphized (d) for all types of trimers, α-β-γ (α, β, γ = G or T standing for Ge or Te) with bond length smaller than 3.6 Å, analyzed from their respective MD simulations at T=300 K over 3 ps. Vertical dashed lines indicate octahedral (90°) and tetrahedral (109.47°) values.

Figure S5 shows the angular distributions (AD) of the as-grown, the modified, the crystalline, and the amorphized phases for any types of trimers, $\alpha-\beta-\gamma\,(\alpha,\beta,\gamma =$ Ge or Te), analyzed from their respective MD simulations at $T = 300\ K$ over 3 ps. Similar to our RDF analysis in Fig. 3, the AD of the as-grown phase was almost identical to that of the modified one except that the latter structure contains a little less tetrahedral bonds than the former one. Compared to the crystalline phase, which contains a major peak around $90°$ and a minor peak just below $180°$ as depicted in Fig. S5 (c), these two amorphous phases reveal much broader peaks around $90°$ indicating an emergence of a significant portion of tetrahedral bonds, in which their bond angles were around $109.47°$. The Ge-centered tetrahedral bonds are contributed mainly by the Te-Ge-Ge and the Te-Ge-Te trimers verifying the central

Ge atom enclosed by $GeTe_3$. An existence of unusual peaks around 50° implies a possible existence of triangular bonds.

The AD of the amorphized phase looks similar to those of the as-grown and the modified phases at a glance. However there are subtle, but significant differences as shown in Figure S3(d). The peak around 90° and the AD values just below 180° begin to become higher than the other two amorphous phases, and the weight around the tetrahedral bond at around 109.47° becomes weakened, meaning the presence of more octahedral-like or pyramidal bonds and less tetrahedral bonds. Moreover, we found that it is more difficult to identify Ge-centered tetrahedral local structures in the amorphized phase than in the other amorphous phases.

References

1. **K. S. Andrikopoulos, S. N. Yannopoulos, G. A. Voyiatzis, A. V. Kolobov, M. Ribes and J. Tominaga, J Phys-Condens Mat 18 (3), 965 (2006).**
2. **R. De Bastiani, E. Carria, S. Gibilisco, M. G. Grimaldi, A. R. Pennisi, A. Gotti, A. Pirovano, R. Bez and E. Rimini, Phys Rev B 80 (24) (2009).**
3. **G. Bunker, Nucl Instrum Methods 207 (3), 437 (1983).**
4. **A. Barranco, F. Yubero, J. P. Espinos, J. P. Holgado, A. Caballero, A. R. Gonzalez-Elipe and J. A. Mejias, Vacuum 67 (3-4), 491 (2002).**
5. **A. V. Kolobov, P. Fons, A. I. Frenkel, A. L. Ankudinov, J. Tominaga and T. Uruga, Nat Mater 3 (10), 703 (2004).**
6. **A. V. Kolobov, P. Fons, J. Tominaga, A. L. Ankudinov, S. N. Yannopoulos and K. S. Andrikopoulos, J Phys-Condens Mat 16 (44), S5103 (2004).**
7. **S. J. Park, M. H. Jang, S. J. Park, M. Ahn, D. B. Park, D. H. Ko and M. H. Cho, J Mater Chem 22 (32), 16527 (2012).**
8. **M. Krbal, A. V. Kolobov, P. Fons, J. Tominaga, S. R. Elliott, J. Hegedus and T. Uruga, Phys Rev B 83 (5) (2011).**